

# High-Pressure, High-Temperature Synthesis and Characterization of Boron Suboxide (B<sub>6</sub>O)

Hervé Hubert,<sup>\*,†</sup> Laurence A. J. Garvie,<sup>‡</sup> Bertrand Devouard,<sup>‡,§</sup> Peter R. Buseck,<sup>‡</sup> William T. Petuskey,<sup>†</sup> and Paul F. McMillan<sup>†</sup>

Department of Chemistry & Biochemistry and Department of Geology,  
Arizona State University, Tempe, Arizona 85287

Received June 16, 1997. Revised Manuscript Received February 16, 1998

Boron suboxide, nominally B<sub>6</sub>O, was synthesized by reducing B<sub>2</sub>O<sub>3</sub> with B up to 10 GPa in a multianvil press at temperatures between 1200 and 1800 °C. The samples were characterized by powder X-ray diffraction, scanning electron microscopy, transmission electron microscopy, and parallel electron energy-loss spectroscopy (PEELS). We used high-pressure techniques to synthesize boron suboxide of improved purity and crystallinity and less oxygen-deficient (i.e., closer to the nominal B<sub>6</sub>O composition) in comparison to products of room-pressure syntheses. We describe the preparation of grains ranging from 20 nm to 40 μm in diameter, as well as the first synthesis of micrometer-sized B<sub>6</sub>O icosahedral twins and euhedral “crystals”. The best materials are obtained for starting mixtures containing an excess B<sub>2</sub>O<sub>3</sub> reacted at 1700–1800 °C between 4 and 5.5 GPa. After the products were washed in water, well-crystallized single-phase product dominated by icosahedrally twinned particles to 30 μm in diameter was easily recovered. Oxygen occupancies ascertained from Rietveld refinements show data consistent with the chemical compositions determined by PEELS. These results give a composition of B<sub>6</sub>O<sub>0.77</sub> for our room-pressure material. The highest O occupancy, B<sub>6</sub>O<sub>0.96</sub>, is obtained for the micrometer-size icosahedral particles prepared at 1700 °C between 4 and 5.5 GPa.

## Introduction

The first laboratory synthesis of diamond in 1954<sup>1</sup> triggered extensive efforts to design and develop materials with a combination of properties approaching or even improving upon those of diamond. Boron-rich solids provide good candidates. They give rise to a large family of refractory compounds with unique crystal structures and a range of interesting physical and chemical properties related to their short interatomic bond lengths and their strongly covalent character.<sup>2,3</sup> Boron-rich phases with a structure based on that of α-rhombohedral B (α-rh B) include boron carbide and boron suboxide (nominally B<sub>6</sub>O), which combine high hardness with low density and chemical inertness, making them useful as abrasives and for other high-wear applications. In addition, these compounds have potentially useful thermal and electronic properties for high-temperature thermoelectric power generation.<sup>4</sup> Boron suboxide qualifies as a “superhard phase”,<sup>5,6</sup>

having a microhardness of 38 GPa<sup>5,7</sup> and abrading properties comparable to that of diamond.<sup>5</sup> Some studies report boron suboxide harder than boron carbide<sup>7</sup> whereas others report the opposite.<sup>8</sup>

The B<sub>6</sub>O structure (space group *R*3̄*m*) consists of eight B<sub>12</sub> icosahedral units situated at the vertexes of a rhombohedral unit cell. The structure can be viewed as a distorted cubic close packing (ccp) of B<sub>12</sub> icosahedra. Two O atoms are located in the interstices along the [111] rhombohedral direction (Figure 1). The O–O distance of 0.307 nm precludes direct O–O bonding.<sup>9</sup>

The study of the properties of B<sub>6</sub>O have been impeded by the fact that pure material with a high degree of crystallinity is difficult to synthesize. In addition, quantitative analysis of compounds containing light elements poses an experimental challenge via traditional analysis techniques such as electron microprobe analysis (EMPA), especially for fine-grained heterogeneous samples. The formation of B<sub>6</sub>O at room pressure was studied previously by several authors.<sup>7,10–12</sup> All

\* To whom correspondence should be addressed.

<sup>†</sup> MRSEC, Department of Chemistry & Biochemistry, Arizona State University.

<sup>‡</sup> Departments of Geology and Chemistry & Biochemistry, Arizona State University.

<sup>§</sup> Present address: Département de Géologie, UMR 6254 Magmas et Volcans, 5, rue Kessler, F-63038 Clermont-Ferrand, France.

(1) Bundy, F. P.; Hall, H. T.; Strong, H. M.; Wentorf, R. H. *Nature* **1955**, *176*, 51.

(2) Lundström, T.; Andreev, Y. G., *Mater. Sci. Eng.* **1996**, *A209*, 16.

(3) Lundström, T.; Bolmgren, H. In *11th International Symposium on Boron, Borides and Related Compounds*; Uno, R., Higashi, I., Eds.; JJAP Series: Tsukuba, 1994; Vol. 10, p 1.

(4) Emin, D. In *Materials Research Society Symposia Proceedings*; Emin, D., Aselage, T. L., Wood, C., Eds.; MRS: Pittsburgh, 1987; Vol. 97, p 3.

(5) Ellison Hayashi, C.; Emond, G. T.; Kuo, S. Y. Abrasion of surfaces with boron suboxide. U.S. Patent 920357, 1994.

(6) Badzian, A. R. *Appl. Phys. Lett.* **1988**, *53*, 2495.

(7) Rizzo, H. F.; Simmons, W. C.; Beilstein, H. O. *J. Electrochem. Soc.* **1962**, *109*, 1079.

(8) Bairamashvili, I. A.; Kalandadze, G. I.; Eristavi, A. V.; Jobava, J. S.; Chotulidi, V. V.; Saloev, Y. I. *J. Less-Common Met.* **1979**, *67*, 455.

(9) Kobayashi, M.; Higashi, I.; Brodhag, C.; Thévenot, F. *J. Mater. Sci.* **1993**, *28*, 2129.

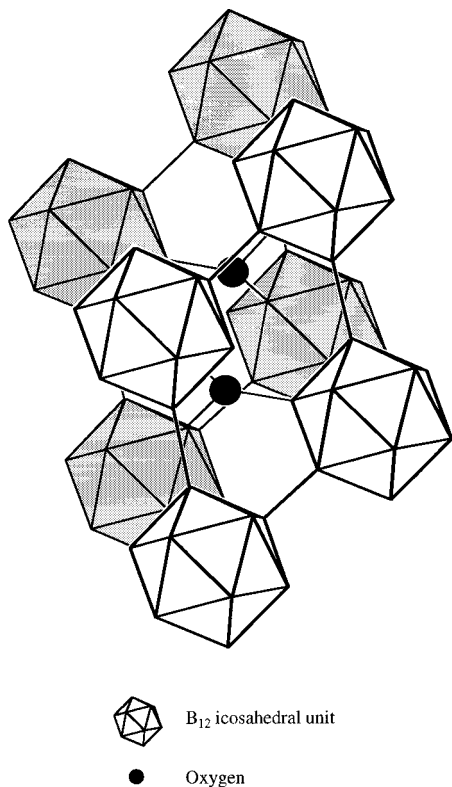


**Figure 1.** Structure of B<sub>6</sub>O built of eight icosahedra at the apices of the rhombohedral unit cell. Gray icosahedra are in the background. The icosahedra are composed of 12 B atoms situated at the corners of a slightly distorted icosahedron. Oxygen atoms are three-coordinated to boron atoms in separate icosahedra in the (001) plane (hexagonal setting).

syntheses produced fine powders with some secondary amorphous products. Sintered ceramics have also been prepared by hot-pressing,<sup>7,11,13</sup> but to our knowledge, no single crystals were obtained. Although boron suboxide is reported as the nominal composition B<sub>6</sub>O,<sup>7,10,12</sup> it is now widely accepted to be nonstoichiometric, and the reported compositions range from B<sub>6</sub>O<sub>0.72</sub> to B<sub>6</sub>O<sub>0.86</sub> (B<sub>7</sub>O).<sup>2,3,11,14–16</sup> La Placa and Post<sup>14</sup> indexed the powder X-ray diffraction (XRD) pattern of B<sub>6</sub>O on the basis of a rhombohedral cell. Its structure was first refined from powder XRD data assuming complete O occupancy.<sup>10,12</sup> However, subsequent refinements revealed a partial O site occupancy ranging from 0.72 to 0.84.<sup>2,3,9</sup> Thus, the formula is best reported as B<sub>6</sub>O<sub>1-x</sub> rather than B<sub>y</sub>O (y > 6). For brevity, we use the nominal formula “B<sub>6</sub>O” in this manuscript, except when the stoichiometry is discussed.

In this investigation, we synthesized B<sub>6</sub>O at high pressure and high temperature (HP–HT) with the goal

(10) Higashi, I.; Kobayashi, M.; Bernhard, J.; Brodhag, C.; Thévenot, F. In *Boron-Rich Solids, A.I.P. Conference and Proceedings*; Emin, D., Aselage, T., Beckel, C. L., Howard, I. A., Wood, C., Eds.; American Institute of Physics: New York, 1991; Vol. 231, p 201.

(11) Petrak, D. R.; Ruh, R.; Goosey, B. F. In *5th Materials Research Symposium*; NBS Spec. Pub.: 1972; Vol. 364, p 605.

(12) Bolmgren, H.; Lundström, T.; Okada, S. In *Boron-Rich Solids, A.I.P. Conference and Proceedings*; Emin, D., Aselage, T., Beckel, C. L., Howard, I. A., Wood, C., Eds.; American Institute of Physics: New York, 1991; Vol. 231, p 197.

(13) Brodhag, C.; Thévenot, F. *J. Less-Common Met.* **1986**, *117*, 1.

(14) LaPlaca, S.; Post, B. *Planseeber. Pulvermet.* **1961**, *9*, 109.

(15) Pasternak, R. A. *Acta Crystallogr.* **1959**, *12*, 612.

(16) Liu, X.; Zhao, X.; Hou, W.; Su, W. *J. Alloys Compd.* **1995**, *223*, L5.

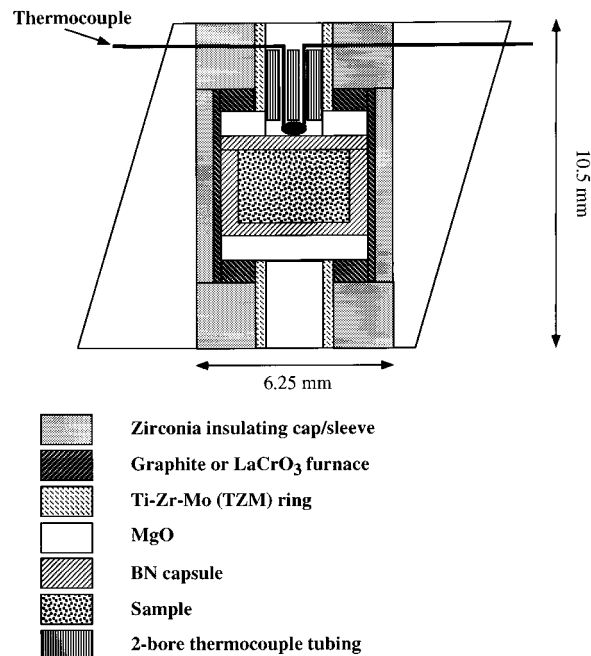


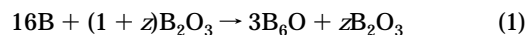
**Figure 2.** Cell assembly containing the B and B<sub>2</sub>O<sub>3</sub> mixture. This 6.25 × 10.5 mm<sup>2</sup> assembly is placed at the center of an MgO octahedron to which pressure is applied isostatically.

of obtaining purer and better crystallized samples. Parallel electron energy-loss spectroscopy (PEELS) was used to determine the B/O ratios of selected run products. The high spatial resolution of PEELS combined with transmission electron microscopy (TEM) provides compositional and structural information at the nanometer scale. Oxygen occupancy was obtained by XRD Rietveld refinement and compared to the chemical compositions obtained using PEELS.

## Experimental Section

**Synthesis.** The HP–HT syntheses were performed using a Walker-type multianvil apparatus.<sup>17,18</sup> The pressure medium consisted of a cast MgO octahedron, and force was applied by eight tungsten carbide cubes with corners truncated to triangular faces. The cell assembly is illustrated in Figure 2.

Amorphous B (claimed purity 99.999%, Aldrich) was mixed with B<sub>2</sub>O<sub>3</sub> (claimed purity 99.99%, Aldrich) in various ratios according to



The mixture, pressed into a pellet, was enclosed in a capsule made of hexagonal BN and placed inside a graphite resistance furnace in the high-pressure cell assembly. The capsule is 3.2 mm in diameter and 3.2 mm high, and it typically holds 30 mg of the B and B<sub>2</sub>O<sub>3</sub> mixture. Samples were pressurized to between 1 and 10 GPa and then heated at 1200–1800 °C from a few minutes to a several hours (Table 1). A LaCrO<sub>3</sub> furnace was used instead of graphite for experiments at 10 GPa and above 1200 °C. Temperature inside the cell was calibrated with Pt/Pt-10%Rh or W-5%Re/W-25%Re thermocouples. A room-pressure sample was prepared at 1400 °C for 8 h under inert atmosphere (argon). The starting material (16B + 2B<sub>2</sub>O<sub>3</sub>) was heated in a crucible made of hexagonal BN.

(17) Walker, D.; Carpenter, M. A.; Hitch, C. M. *Am. Mineral.* **1990**, *75*, 1020.

(18) Leinenweber, K.; Parise, J. *J. Solid State Chem.* **1985**, *114*, 277.

**Table 1. Summary of Selected Runs Prepared between Room Pressure and 10 GPa and from 1200 to 1800 °C<sup>a</sup>**

| run | initial mixture<br>B <sub>2</sub> O <sub>3</sub> :16B | P<br>(GPa) | T<br>(°C) | time<br>(min) | products  | particles morphologies                        |                    |                                 |
|-----|---|------------|-----------|---------------|---|---|--------------------|---------------------------------|
|     |   |            |           |               |   | SEM <sup>c,e</sup>                            | TEM <sup>d,e</sup> | optical microscopy <sup>f</sup> |
| RP1 | 2   | 1 atm      | 1400      | 480           | B <sub>6</sub> O + B <sub>2</sub> O <sub>3</sub> (s) + am     | fine irregular euh                            | euh (to 1 μm)      | Br powder                       |
| 642 | 1   | 2          | 1700      | 30            | B <sub>6</sub> O + aph  | sintered fine grains                          | euh < 1 μm         | R-Br                            |
| 679 | 1.5   | 2          | 1700      | 30            | B <sub>6</sub> O + B <sub>2</sub> O <sub>3</sub> (s) + am     | sintered fine grains                          | euh >> icos        | R-Br                            |
| 656 | 1.2   | 3          | 1700      | 30            | B <sub>6</sub> O + B <sub>2</sub> O <sub>3</sub> (s) + am     | sintered fine grains                          | euh >> icos        | R-Br                            |
| 667 | 1.1   | 4          | 1700      | 30            | B <sub>6</sub> O + B <sub>2</sub> O <sub>3</sub> (s)          | icos in sintered fine<br>grained matrix       | euh > icos         | dark R icos                     |
| 672 | 2   | 4          | 1700      | 120           | B <sub>6</sub> O + B <sub>2</sub> O <sub>3</sub> (s)          | icos (to 30 μm) >><br>euh crystals (to 40 μm) | euh > icos         | dark R icos >> O-R euh          |
| 423 | 4   | 5          | 1800      | 30            | B <sub>6</sub> O + B <sub>2</sub> O <sub>3</sub> (s)          | icos (0.1–5 μm)                               | icos. (to 1 μm)    | O-R icos >> dark R icos         |
| 558 | 1   | 5.5        | 1700      | 30            | B <sub>6</sub> O + B <sub>2</sub> O <sub>3</sub> (s) + am     | icos (to 20 μm)                               | euh > icos         | O-R icos >> dark R icos         |
| 620 | 1.05  | 5.5        | 1700      | 30            | B <sub>6</sub> O + B <sub>2</sub> O <sub>3</sub> (s)          | icos (to 20 μm)                               | icos >> euh        | O-R icos >> dark R icos         |
| 653 | 1.2   | 5.5        | 1700      | 30            | B <sub>6</sub> O + B <sub>2</sub> O <sub>3</sub> (s)          | icos (to 10 μm)                               | icos >> euh        | O-R icos >> dark R icos         |
| 451 | 2   | 5.5        | 1800      | 5             | B <sub>6</sub> O + B <sub>2</sub> O <sub>3</sub> (s)          | euh > icos (to 1 μm)                          | icos > euh         | O-R powder                      |
| 555 | 1   | 7.5        | 1700      | 30            | B <sub>6</sub> O + am   | sintered fine grains > icos                   | euh > icos         | O-R powder                      |
| 488 | 4   | 7.5        | 1700      | 30            | B <sub>6</sub> O + B <sub>2</sub> O <sub>3</sub> <sup>b</sup> | icos (1–3 μm)                                 | icos (to 1 μm)     | O-R icos                        |
| 396 | 4   | 10         | 1200      | 180           | B <sub>2</sub> O <sub>3</sub> <sup>b</sup> + B <sub>6</sub> O | sintered fine grains                          | euh                | O-R powder                      |
| 404 | 1   | 10         | 1600      | 20            | B <sub>6</sub> O + am   | sintered fine grains                          | euh                | O-R powder                      |
| 401 | 4   | 10         | 1800      | 5             | B <sub>6</sub> O + B <sub>2</sub> O <sub>3</sub> <sup>b</sup> | sintered fine grains ><br>euh (1–10 μm)       | μm-sized euh       | O-R powder                      |

<sup>a</sup> The products determined using XRD and PEELS are listed in order of decreasing abundance. <sup>b</sup> B<sub>2</sub>O<sub>3</sub> polymorphs; am, amorphous phase (minor amounts); (s), water-soluble boron oxide(s). <sup>c</sup> SEM observation of the coarse part of the sample. <sup>d</sup> TEM observation of the fine part of the sample. <sup>e</sup> >, abundance; euh, euhedral grains; icos, icosahedral grains. <sup>f</sup> Br, brown; R, red; R-Br, reddish-brown; O-R, orange-red.

**Characterization Techniques.** The recovered capsule and cell assembly were broken apart and initially examined using optical microscopy. A portion of the sample was gently ground between two WC cubes and deposited on a single-crystal, low-background quartz slide for analysis by powder XRD. A Siemens D5000 powder X-ray diffractometer, employing Cu Kα radiation and in a  $\theta$ - $2\theta$  configuration, was used to determine the different materials present. Unit cells and O site occupancy were derived from Rietveld refinements (of selected samples) obtained using the General Structure Analysis System (GSAS) computer program (Larson and VonDreele, Los Alamos National Laboratory). NaCl was used as an internal standard.

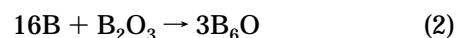
Samples for PEELS were prepared by crushing a small amount of material in methanol and allowing the fine mineral suspension to dry on a lacy-carbon TEM grid. Spectra were obtained using a Philips 400ST-FEG TEM operated at an accelerating voltage of 100 keV. The TEM was operated with a cold field-emission gun providing an energy resolution of about 0.7 eV, as measured at the zero-loss peak. Spectra were acquired with a Gatan 666 PEELS from thin regions, typically 20 nm thick or less, overhanging holes in the lacy-carbon film. The spectra were analyzed with the Gatan el/p EELS software, and the elemental ratios determined using Hartree-Slater cross sections. For quantitative analysis, spectra were collected with a spectrometer dispersion of 1 eV and acquisition times of 2–4 s. The morphologies and particle sizes of the samples were studied by scanning electron microscopy (SEM) and TEM. The SEM samples were gold-coated and imaged with a JEM-5800 operated at 8 keV. The high-resolution TEM samples were prepared as described for the PEELS analysis and were observed on a Topcon 002B operated at 200 keV, which allows a point-to-point resolution down to 0.19 nm.

## Results and Discussion

**Run Products.** The results of the reduction of B<sub>2</sub>O<sub>3</sub> by B are summarized in Table 1. Many samples effervesced vigorously in water, leaving B<sub>6</sub>O as the only insoluble product. Under the binocular microscope, some samples appeared coarsely crystalline, whereas others had a dull chalky luster. The samples varied from brown (room pressure) to orange-red (high pressure). The reduction of B<sub>2</sub>O<sub>3</sub> by B leads to the formation of B<sub>6</sub>O according to

**Table 2. List of Observed Reflections for B<sub>6</sub>O (Sample 451, Space Group R3̄m, Hexagonal Axis)**

| <i>h</i> | <i>k</i> | <i>l</i> | <i>d</i> -spacing<br>(Å) | intensity<br>( <i>I</i> / <i>I</i> <sub>0</sub> ) |
|----------|----------|----------|--------------------------|---|
| 1        | 0        | 1        | 4.363                    | 14  |
| 0        | 0        | 3        | 4.106                    | 71  |
| 0        | 1        | 2        | 3.719                    | 17  |
| 1        | 1        | 0        | 2.694                    | 10  |
| 1        | 0        | 4        | 2.570                    | 100   |
| 0        | 2        | 1        | 2.292                    | 65  |
| 1        | 1        | 3        | 2.252                    | 2   |
| 0        | 1        | 5        | 2.180                    | 7   |
| 2        | 0        | 4        | 1.860                    | 6   |
| 2        | 1        | 1        | 1.748                    | 3   |
| 2        | 0        | 5        | 1.695                    | 4   |
| 1        | 0        | 7        | 1.648                    | 5   |
| 1        | 1        | 6        | 1.634                    | 4   |
| 0        | 1        | 8        | 1.463                    | 9   |
| 3        | 0        | 3        | 1.455                    | 8   |
| 2        | 1        | 5        | 1.435                    | 10  |
| 0        | 2        | 7        | 1.405                    | 3   |
| 2        | 2        | 0        | 1.347                    | 7   |
| 2        | 0        | 8        | 1.286                    | 5   |
| 1        | 3        | 1        | 1.280                    | 6   |
| 2        | 2        | 3        | 1.267                    | 4   |
| 2        | 1        | 7        | 1.246                    | 4   |
| 3        | 1        | 4        | 1.193                    | 3   |
| 2        | 1        | 8        | 1.160                    | 3   |
| 4        | 0        | 2        | 1.146                    | 4   |



Powder XRD shows that B<sub>6</sub>O (Tables 1, 2 and Figure 3a) formed over the whole pressure and temperature range of our investigation. In addition, both low-pressure hexagonal B<sub>2</sub>O<sub>3</sub> I<sup>19</sup> and high-pressure orthorhombic B<sub>2</sub>O<sub>3</sub> II<sup>20</sup> were identified together with amorphous material and at least one HBO<sub>2</sub> polymorph.<sup>21</sup> The amorphous material was evident as two broad humps centered around 22.5° and 37°  $2\theta$  Cu Kα, as observed in the powder XRD patterns (Figure 3b).

(19) Gurr, G. E.; Montgomery, P. W.; Knutson, C. D.; Gorres, B. T. *Acta Crystallogr.* **1970**, *B26*, 906.

(20) Prewitt, C. T.; Shannon, R. D. *Acta Crystallogr.* **1968**, *B24*, 868.

(21) Zachariasen, W. H. *Acta Crystallogr.* **1963**, *16*, 380.

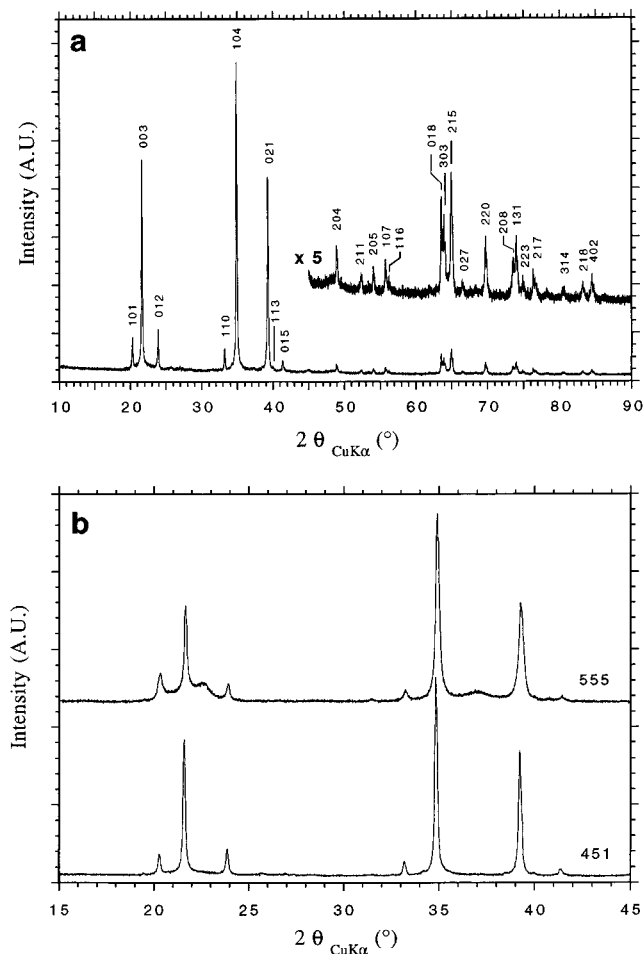


**Figure 3.** Powder X-ray diffraction patterns for B<sub>6</sub>O. (a) XRD pattern of washed sample 451. (b) Comparison of samples 555 and 451 showing the presence of amorphous material in 555. (A.U. = arbitrary units).

The B:O ratios of the compounds were determined using PEELS (Figure 4) and confirmed the results obtained by XRD. The shape of the B K-edge is characteristic of the B chemical environment and gives a “fingerprint” of the different compounds. Figure 4 shows the B K-edges of  $\beta$ -rhombohedral B ( $\beta$ -rh B),  $\alpha$ -rh B, glassy B<sub>2</sub>O<sub>3</sub>, and four of the run products. The B K-edge from  $\alpha$ -rh B is shown for comparison. The edge shapes for glassy and orthorhombic B<sub>2</sub>O<sub>3</sub> (B<sub>2</sub>O<sub>3</sub> II) are consistent with published PEELS data.<sup>22,23</sup> The B K-edge of glassy B<sub>2</sub>O<sub>3</sub> is similar to that of compounds containing 3-fold-coordinated B, and the B<sub>2</sub>O<sub>3</sub> II with 4-fold-coordinated B.<sup>23</sup> The B K-edge shape of B<sub>6</sub>O is similar to that from other refractory B-rich solids with the  $\alpha$ -rh B structure such as B<sub>6</sub>As and B<sub>6</sub>N<sub>1-x</sub>.<sup>24,25</sup>

For our room-pressure sample (RP1) and for samples prepared at 2 and 3 GPa, B<sub>6</sub>O was identified together with some amorphous material. XRD patterns of these samples show the pattern for B<sub>6</sub>O together with two broad humps centered around 22.5° and 37° 2 $\theta$  Cu K $\alpha$

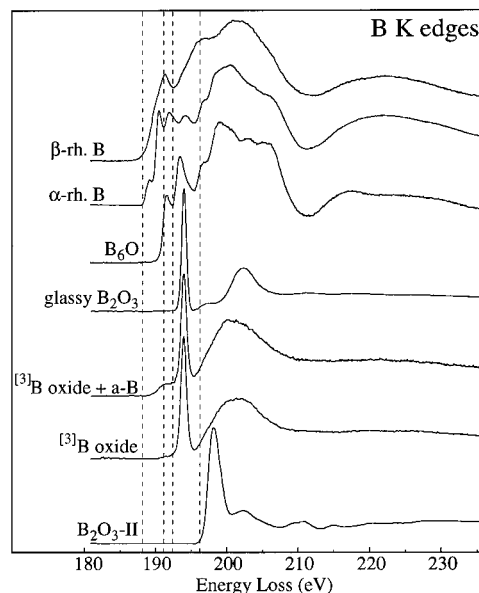


**Figure 4.** PEELS B K-edges for the starting materials, glassy B<sub>2</sub>O<sub>3</sub>, and  $\beta$ -rhombohedral B ( $\beta$ -rh B). For comparison, the B K-edge of B<sub>6</sub>O is shown with the K-edges of  $\alpha$ -rhombohedral B  $\alpha$ -rh B and the products: an amorphous 3-fold coordinated boron oxide (<sup>10</sup>B oxide) with amorphous boron (a-B), amorphous 3-fold coordinated boron oxide (<sup>10</sup>B oxide), and orthorhombic B<sub>2</sub>O<sub>3</sub> (B<sub>2</sub>O<sub>3</sub> II).

from the amorphous boron material. Similarly, amorphous materials were reported by Brodhag et al.,<sup>13</sup> Kobayashi et al.,<sup>9</sup> and Bolmgren et al.<sup>12</sup>

Well-crystallized B<sub>6</sub>O formed between 4 and 5.5 GPa at 1700 °C for all starting mixtures having a B<sub>2</sub>O<sub>3</sub>/16B ratio greater than 1 (excess B<sub>2</sub>O<sub>3</sub>). After the mixture was washed in water, B<sub>6</sub>O is the only insoluble product (B<sub>2</sub>O<sub>3</sub> I is water-soluble) as shown by the XRD pattern of sample 451 (Figure 3a). Well-crystallized B<sub>6</sub>O and a small quantity of amorphous material formed for syntheses prepared according to eq 2.

Between 7.5 and 10 GPa and with excess B<sub>2</sub>O<sub>3</sub>, well-crystallized B<sub>6</sub>O and both B<sub>2</sub>O<sub>3</sub> polymorphs formed. The B<sub>6</sub>O cannot be separated from B<sub>2</sub>O<sub>3</sub> II by washing in water since the latter is insoluble. Without excess B<sub>2</sub>O<sub>3</sub> (run 555), B<sub>6</sub>O is produced along with some amorphous material. The two broad features present in the powder XRD pattern of sample 555 (Figure 3b) are similar to the ones described in the two previous paragraphs.

**Morphology.** Grain morphologies of selected samples were characterized using SEM and TEM (Table 1). Grains larger than 1  $\mu$ m can be divided into several types: multiply twinned icosahedral particles, euhedral (trigonal) grains, intergrown subhedral to anhedral icosahedral grains, and rounded anhedral sintered masses formed of submicron grains.

The room-pressure sample consists of fine euhedral nonsintered particles ( $\leq 1 \mu$ m). At 2 and 3 GPa, the products are dominated by submicron euhedral grains with some sintered masses. TEM observations also reveal euhedral particles with a few nanometer-sized icosahedra. At 5.5 GPa, 1700 °C, and B<sub>2</sub>O<sub>3</sub>/16B of 1, micrometer-sized particles of B<sub>6</sub>O formed in a water-soluble matrix together with microcrystalline B<sub>6</sub>O (Figures 5). Translucent and orange-red grains are observed in reflected and transmitted light along with a few dark-red ones (Figure 6a). The color is consistent

(22) Garvie, L. A. J.; Buseck, P. R.; Craven, A. J. *Can. Mineral.* **1995**, *33*, 1157.

(23) Garvie, L. A. J.; Craven, A. J.; Brydson, R. *Am. Mineral.* **1995**, *80*, 1132.

(24) Hubert, H.; Garvie, L. A. J.; Buseck, P. R.; Petuskey, W. T.; McMillan, P. F. *J. Solid State Chem.* **1998**, *133*, 356.

(25) Garvie, L. A. J.; Hubert, H.; Buseck, P. R.; Petuskey, W. T.; McMillan, P. F. *J. Solid State Chem.* **1998**, *133*, 365.

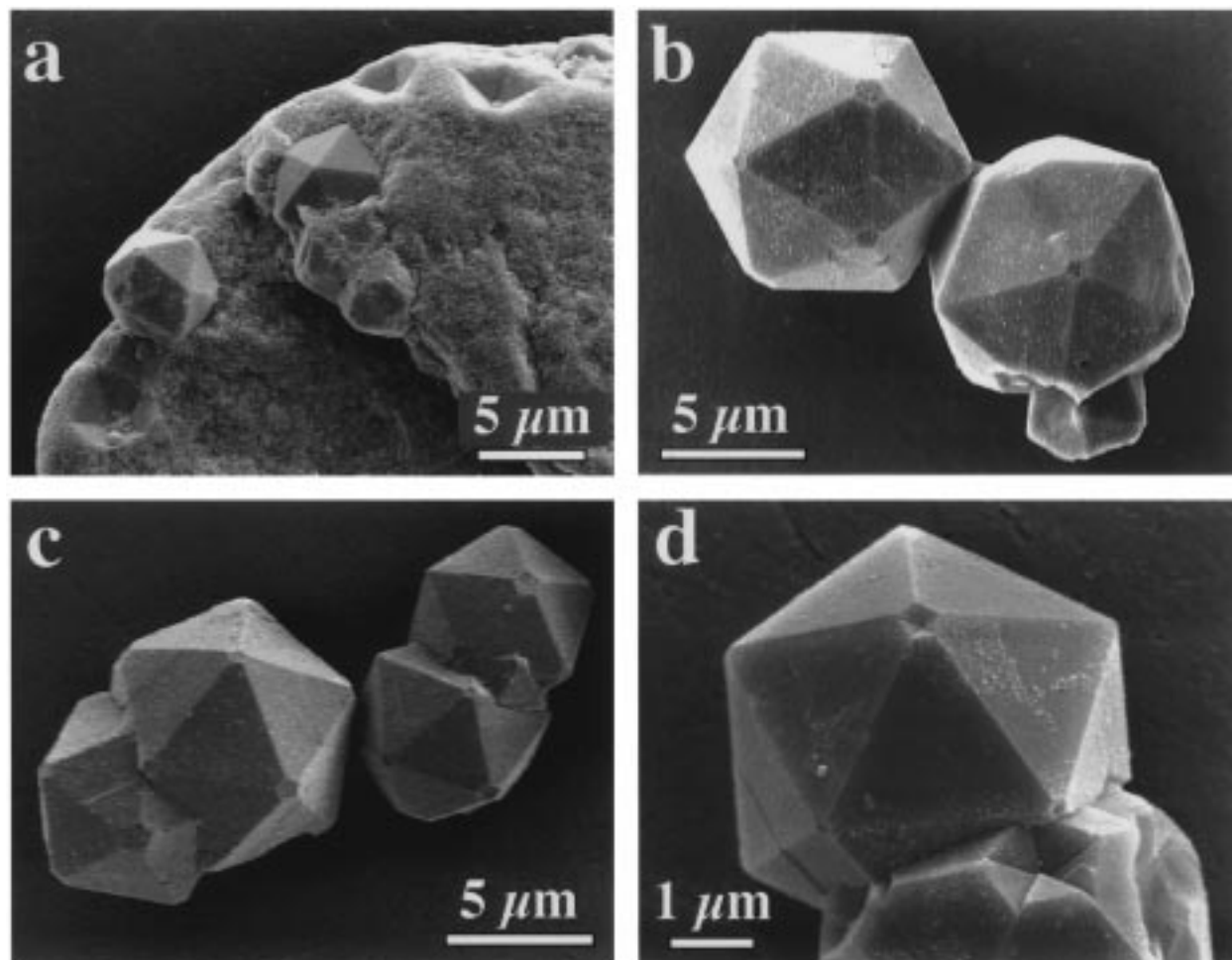


**Figure 5.** SEM pictures of  $B_6O$  icosahedra (multiply twinned particles, MTPs) of run 558. (a) Icosahedral particles in a fine-grained matrix of  $B_6O$ . (b) Two icosahedra free of matrix, one oriented along a 3-fold axis, and the other along a 5-fold axis. (c) Intergrown icosahedra. (d) MTPs showing well-developed reentrant angles at the apexes, indicative of twinning.

with a band gap around 2 eV.<sup>26</sup> Similar crystals formed with excess  $B_2O_3$  and similar run conditions. The particles formed as near-perfect icosahedra to 20  $\mu m$  in size (Figure 5); no other morphologies were observed for grains over 1  $\mu m$ . Micrometer-sized icosahedra (to 30  $\mu m$  for run 672) also formed at 4 GPa. Most are dark red with a few red-orange ones. A few translucent red-orange euhedral crystals ("trigonal platelets") to 40  $\mu m$  were also recovered (Figure 6b). At 7.5 GPa, sintered icosahedral grains (to 3  $\mu m$ ) occur with  $B_2O_3$  II, whereas samples recovered from 10 GPa only show euhedral particles by SEM and TEM. Well-crystallized samples of  $B_6O$  with the largest "crystal" sizes are obtained for pressures between 4 and 5.5 GPa at 1700 °C. Larger particles sizes are obtained for the lowest excess flux ( $B_2O_3$ ). The parameters controlling the predominance of a certain morphology over another is not yet well understood.

The icosahedral morphology of these  $B_6O$  grains is highly unusual. They are not single crystals (which would be incompatible with the  $R\bar{3}m$  space group) but are multiply twinned particles associating twenty individuals whose growth is favored by the particular geometry of the  $B_6O$  structure and the experimental synthesis conditions.<sup>27</sup> Imperfect boron carbide ico-

hedral twins were also observed in chemical vapor deposited experiments.<sup>28,29</sup>

For most runs, the fine-grain fraction ( $\ll 1 \mu m$ ) is dominated by well-sorted euhedral to subhedral particles from 20 to 100 nm in diameter (Figure 7a). Twinning is common, either along a single set of parallel planes or along all equivalent  $\{100\}$  planes (rhombohedral axes). The first case results in euhedral faulted crystals (Figure 7b), whereas the second leads to the formation of multiply twinned icosahedral particles, as described above. Both types of twinning occurs in the fine-grained fraction of the same sample, but intermediate types (i.e., twinning of a small number of individuals along nonparallel planes) are rarely observed. Twin boundaries and isolated stacking faults correspond to an inversion in the ...A-B-C-A-B-C... stacking sequence for the cubic close packing (ccp) of  $B_{12}$  units, resulting locally in a hexagonal close packed (hcp)-like stacking (...A-B-A...) around the planar defect. Faceted voids, a few nanometer in size, were present on some nanometer-sized  $B_6O$  grains. Similar twinning patterns, stacking faults, and voids were reported in boron carbides.<sup>30,31</sup>

(26) Lee, S.; Kim, S. W.; Bylander, D. M.; Kleinman, L. *Phys. Rev.* **1991**, *B44*, 3550.

(27) Hubert, H.; Devouard, B.; Garvie, L. A. J.; O'Keeffe, M.; Buseck, P. R.; Petuskey, W. T.; McMillan, P. F. *Nature* **1998**, *391*, 376.

(28) Ploog, K. J. *Less-Common Met.* **1974**, *35*, 131.

(29) Ploog, K. J. *Less-Common Met.* **1973**, *31*, 177.

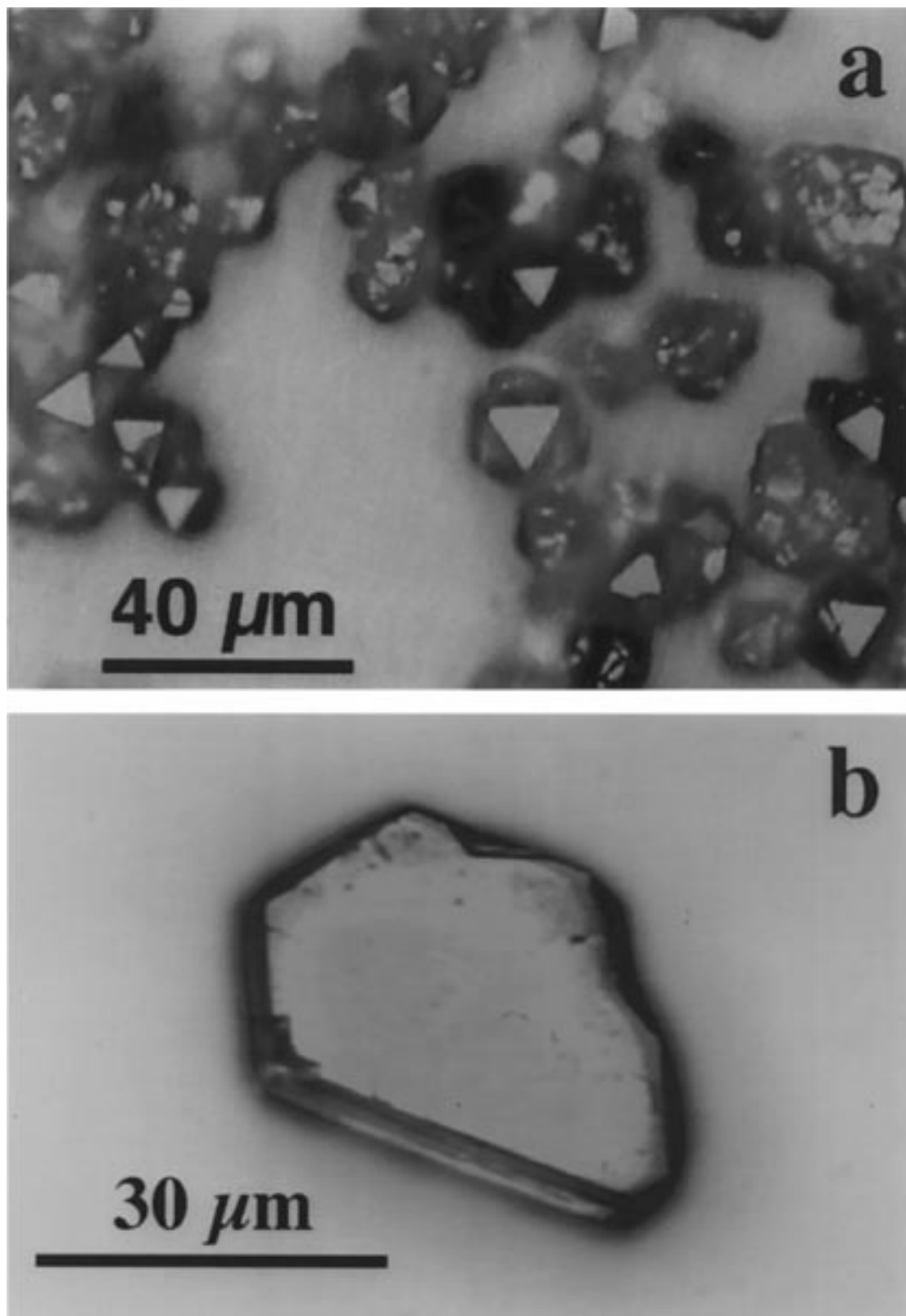


**Figure 6.** Optical images of orange-red B<sub>6</sub>O grains. (a) Triangular faces of individual icosahedra are evident in reflected light (run 653). All single particles are isolated or clustered icosahedra. (b) Euhedral "crystal" (run 672).

**Stoichiometry.** The refined hexagonal cell parameters and O occupancies for B<sub>6</sub>O<sub>1-x</sub> samples 451, 620,

(30) Mackinnon, I. D. R.; Aselage, T.; Van Deusen, S. B. In *Boron-rich solids*, AIP Conference Proceedings; Emin, D., Aselage, T., Beckel, C. L., Howard, I. A., Wood, C., Eds.; American Institute of Physics: New York, 1986; Vol. 140, p 114.

(31) Ashbee, K. H. G. *Acta Metallurg.* 1971, 19, 1079.

and RP1 are given in Table 3 along with published data. The chemical compositions determined by PEELS are consistent with the O occupancy obtained by Rietveld refinements (Table 3). PEELS shows that the room-pressure sample (RP1) has a composition B<sub>6</sub>O<sub>0.73</sub> ( $\sigma = 0.02$ ,  $n = 22$ ) and compares well to the value B<sub>6</sub>O<sub>0.78±0.03</sub> obtained by Rietveld refinement. The cell parameters

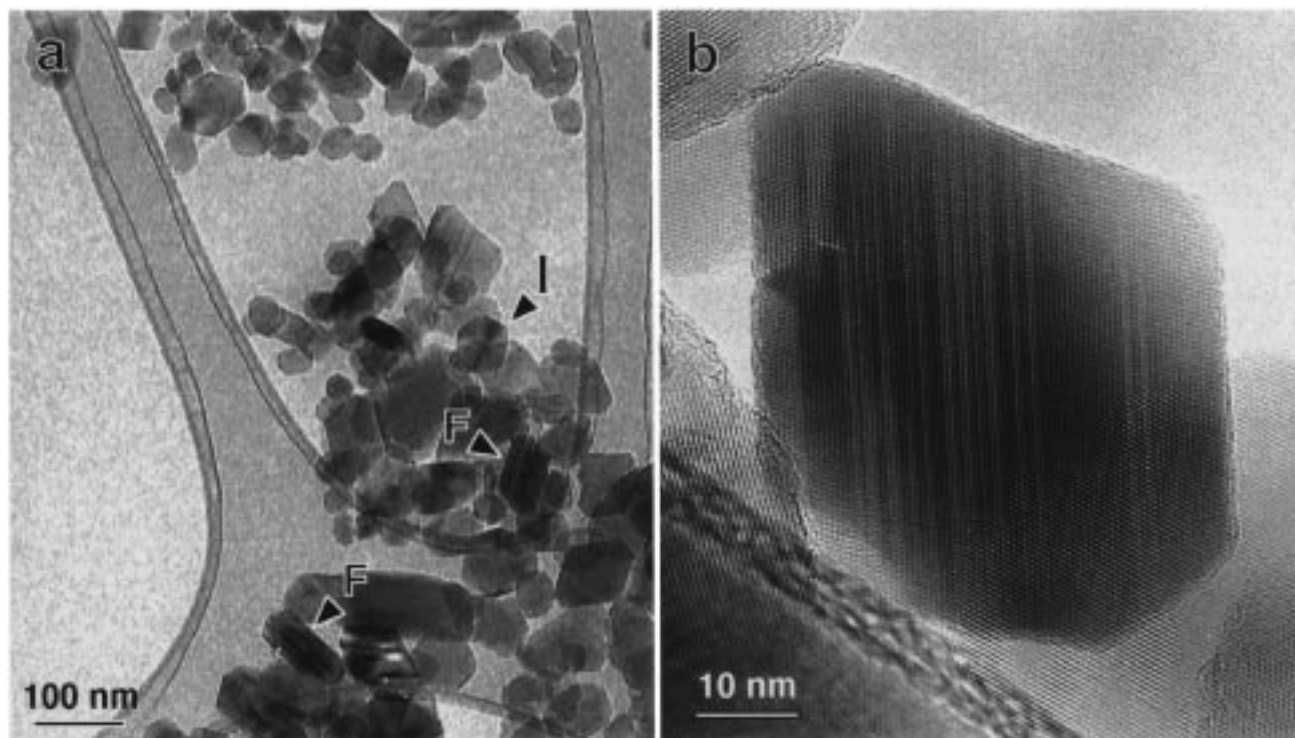


**Figure 7.** TEM pictures of  $B_6O$  crystals. (a) Low magnification showing the euhedral morphologies, with some faulted crystals (F) and icosahedral twins (I). (b) High-resolution picture of a crystal with numerous stacking faults and twin lamellae.

**Table 3.** Cell Parameters for Selected Samples of  $B_6O$  (Space Group  $R\bar{3}m$ , Hexagonal Axes)<sup>a</sup>

| compd          | $a_h$ (Å) | $c_h$ (Å)  | $c_h:a_h$ | $V$ (Å <sup>3</sup> ) | O occupancy        |                  | ref        | preparation method <sup>e</sup> |
|----------------|-----------|------------|-----------|-----------------------|--------------------|------------------|------------|---------------------------------|
|                |           |            |           |                       | XRD                | PEELS            |            |                                 |
| $B_6O_{0.72}$  | 5.361(1)  | 12.340(1)  | 2.301     | 307.14                | 0.72 <sup>c</sup>  | N/A <sup>b</sup> | 3          | RP                              |
| $B_6O_{0.76}$  | 5.367(1)  | 12.328(2)  | 2.297     | 307.53                | 0.76 <sup>c</sup>  | N/A              | 9          | RP                              |
| $B_6O_{0.77}$  | 5.3696(4) | 12.3258(6) | 2.295     | 307.77                | 0.77               | $0.73 \pm 0.02$  | this study | run RP1                         |
| $B_6O_{0.787}$ | 5.3824(4) | 12.322(1)  | 2.289     | 309.15                | 0.787 <sup>c</sup> | N/A              | 2          | RP                              |
| $B_6O_{0.839}$ | 5.3761(7) | 12.326(3)  | 2.293     | 308.52                | 0.839 <sup>c</sup> | N/A              | 2          | RP                              |
| $B_6O_{0.89}$  | 5.3872(1) | 12.3152(3) | 2.286     | 309.53                | 0.89               | $0.90 \pm 0.1$   | this study | run 451                         |
| $B_6O_{0.95}$  | 5.3902(2) | 12.3125(4) | 2.284     | 309.78                | 0.95               | $0.96 \pm 0.08$  | this study | run 620                         |
| $B_6O_x^d$     | 5.3862(3) | 12.319(1)  | 2.287     | 309.51                | N/A                | N/A              | 12         | 6 GPa                           |
| $B_6O_x^d$     | 5.386(3)  | 12.326(4)  | 2.289     | 309.66                | N/A                | N/A              | 11         | hot-P                           |
| $B_6O_x^d$     | 5.395     | 12.342     | 2.288     | 311.10                | N/A                | N/A              | 7          | hot-P                           |
| $B_6O_x^d$     | 5.435     | 12.415     | 2.284     | 317.60                | N/A                | N/A              | 16         | 3.5 GPa                         |

<sup>a</sup> Estimated standard deviations are given in parentheses. O occupancies are derived from Rietveld refinement and PEELS analysis.

<sup>b</sup> Data not available. <sup>c</sup> O occupancy reported in refs 2, 3, and 9. <sup>d</sup> O occupancy was not refined for these samples. <sup>e</sup> RP, samples prepared at room pressure; hot-P, samples prepared by hot-pressing.

( $a_h = 5.3696$  Å,  $c_h = 12.3258$  Å,  $V = 307.77$  Å<sup>3</sup>) and O occupancy of RP1 are consistent with previous refinements.<sup>2,9</sup>

Compared to room-pressure syntheses, HP-HT techniques produce  $B_6O$  closer to the ideal composition. The cell volume and O occupancy for runs 451 and 620 are greater than for our room-pressure sample and the ones reported by other authors.<sup>2,3,9</sup> The largest cell volume ( $a_h = 5.3902$  Å,  $c_h = 12.3125$  Å,  $V = 309.78$  Å<sup>3</sup>) and highest O occupancy (0.95) are obtained for runs containing the largest icosahedral and euhedral "crystals". PEELS gives a similar composition of  $B_6O_{0.96 \pm 0.08}$  ( $\sigma = 0.08$ ,  $n = 18$ ). A sample prepared by Bolmgren et al.<sup>12</sup> at 6 GPa and 1600 °C gives cell parameters ( $a_h = 5.3862$  Å,  $c_h = 12.319$  Å,  $V = 309.51$  Å<sup>3</sup>) comparable to our 5.5 GPa runs although the O content was not determined.

The increase in  $a_h$  and cell volume and decrease in  $c_h$  can be correlated with a higher O content of the  $B_6O_{1-x}$ . Our refinements, together with some previous Rietveld refinements, are in agreement and show linear trends

in  $c_h$ ,  $a_h$ , and cell volume with respect to O occupancy (Figure 8). Most published data are consistent with these variations, although one refinement in which the O occupancy was determined<sup>2</sup> (see Figure 8, open symbol) does not follow these trends. Similarly, the cell volume and lattice constants determined by Rizzo<sup>7</sup> and Petrak<sup>11</sup> for hot-pressed  $B_6O$  are inconsistent with the trends observed in Figure 8. In these two studies, O occupancies were not determined. Liu et al.<sup>16</sup> claimed a new route to prepare boron suboxide, reported as  $B_7O$ , at 3.5 GPa and 1200 °C from B and ZnO. Their cell parameters (Table 3) do not agree with our or published cell refinements. Furthermore, their published XRD pattern does not show the (110) reflection ( $I/I_0 = 10\%$ ) of  $B_6O$  but displays a reflection assigned as (200) ( $d = 2.353$  Å), which is inconsistent with the  $B_6O$  structure.

The trend in cell dimensions with O occupancy is explained using a sphere-packing model. The structure of  $\alpha$ -rh B can be considered as a distorted ccp of icosahedral  $B_{12}$  units<sup>32</sup> and constitutes the basic frame-

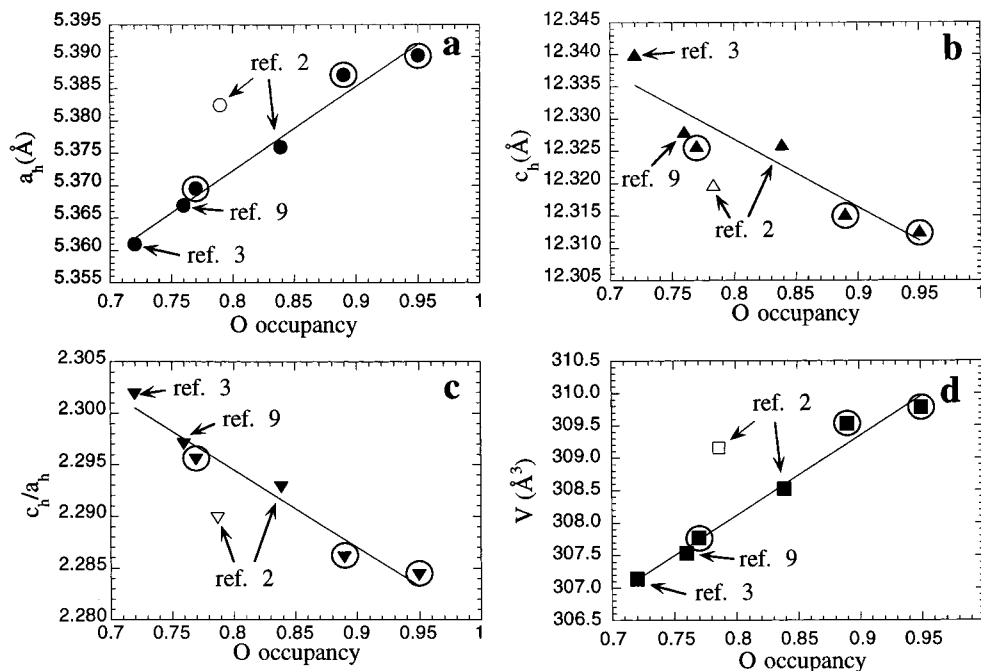


**Figure 8.** Variation of cell dimensions with O occupancy. (a)  $a_h$ :O occupancy. (b)  $c_h$ :O occupancy. (c)  $a_h/c_h$ :O occupancy. (d)  $V$ :O occupancy. (Data points obtained in this study are circled.)

**Table 4. Cell Parameters for Selected Compounds Related to the  $\alpha$ -rh B Structure (Space Group  $R\bar{3}m$ , Hexagonal Axes)**

| compd                            | $a_h$ (Å) | $c_h$ (Å)   | $c_h:a_h$ | $V$ (Å <sup>3</sup> ) | ref        |
|----------------------------------|-----------|-------------|-----------|-----------------------|------------|
| $\alpha$ -rh B                   | 4.927(3)  | 12.564(7)   | 2.550     | 264.13                | 34         |
| B <sub>6</sub> O <sub>0.95</sub> | 5.3902(2) | 12.3125(4)  | 2.284     | 309.78                | this study |
| B <sub>6</sub> N <sub>1-x</sub>  | 5.457(7)  | 12.241(15)  | 2.243     | 315.7                 | 24         |
| B <sub>4</sub> C                 | 5.6039(4) | 12.0786(14) | 2.155     | 328.5                 | 33         |
| B <sub>12</sub> S                | 5.80      | 11.90       | 2.05      | 346.7                 | 35         |
| B <sub>6</sub> P                 | 6.000(4)  | 11.857(8)   | 1.98      | 369.7                 | 34         |
| B <sub>6</sub> As                | 6.169(4)  | 11.900(6)   | 1.93      | 392.2                 | 34         |

<sup>a</sup> The compounds are arranged in order of increasing atomic sizes (of the interstitial atom) going down the table. Estimated standard deviations are given in parentheses.

work for the structure of B<sub>6</sub>O, B<sub>6</sub>N,<sup>24</sup> B<sub>4</sub>C,<sup>33</sup> B<sub>6</sub>P,<sup>34</sup> B<sub>12</sub>S,<sup>35</sup> and B<sub>6</sub>As.<sup>34</sup>  $\alpha$ -rh B<sup>34</sup> has the smallest cell volume with the smallest  $a_h$  and largest  $c_h$  of all  $\alpha$ -rh B-rich compounds (Table 4). Insertion of atoms in the interstitial sites of the close-packed layers (Wyckoff position 6c) results in a cell volume expansion (increase in  $a_h$  and decrease in  $c_h$ ) proportional to the size of the atom occupying these sites. Therefore, in B<sub>6</sub>O<sub>1-x</sub>, cell volume and  $a_h$  are expected to increase (and  $c_h$  to decrease) with

(32) Matkovitch, V. I.; Economy, J. In *Boron and Refractory Borides*; Matkovitch, V. I., Ed.; Springer-Verlag: Berlin, Heidelberg, 1977; p 78.

(33) Larson, A. C. In *Boron-rich solids, AIP Conference Proceedings*; Emin, D., Aselage, T., Beckel, C. L., Howard, I. A., Wood, C., Eds.; American Institute of Physics: New York, 1986; Vol. 140, p 109.

(34) Morosin, B.; Mullendore, A. W.; Emin, D.; Slack, G. A. In *Boron-rich solids, AIP Conference Proceedings*; Emin, D., Aselage, T., Beckel, C. L., Howard, I. A., Wood, C., Eds.; American Institute of Physics: New York, 1986; Vol. 140, p 70.

(35) Matkovitch, V. I. *J. Am. Chem. Soc.* **1961**, *83*, 1804.

the filling of O interstitial sites, i.e., with increasing O occupancy.

## Conclusion

Quantitative analysis shows that samples prepared at high pressure are less O-deficient (i.e., closer to the nominal B<sub>6</sub>O composition) than room-pressure materials. The cell volume refinement (obtained from powder XRD) could be used as a simple tool to estimate the stoichiometry of B<sub>6</sub>O samples.

We believe that this is the first reported synthesis of euhedral and icosahedral micrometer-sized B<sub>6</sub>O "crystals". HP–HT techniques could provide a useful route to well-controlled boron suboxide syntheses (stoichiometry, grain size, and morphology). In particular, the near-spherical morphology of the icosahedral particles (formed under a certain set of pressure–temperature conditions) combined with the high hardness of B<sub>6</sub>O could provide a high-wear material useful for abrasive applications.

**Acknowledgment.** We thank Kurt Leinenweber for helpful discussions and Vincent Gobe and Stéphane F eret for their assistance. This work was supported by NSF Grants MRG DMR-9121570, MRSEC DMR-9632635, EAR-9418206, and EAR-92-19376. The TEM and PEELS used for this research were performed at the Center for High Resolution Electron Microscopy at Arizona State University, established with support from the National Science Foundation (DMR-8913384).

CM970433+